Biochimica et Biophysica Acta 1777 (2008) 496–503

Contents lists available at ScienceDirect

Biochimica et Biophysica Acta

journal homepage: www.elsevier.com/locate/bbabio

Direct quantification of the four individual S states in Photosystem II using EPR spectroscopy

Guangye Han [a], Felix M. Ho [a], Kajsa G.V. Havelius [a], Susan F. Morvaridi [b], Fikret Mamedov [a], Stenbjörn Styring [a,*]

[a] Molecular Biomimetics, Department of Photochemistry and Molecular Science, Ångström Laboratory, P.O. Box 523, Uppsala University, SE-751 20 Uppsala, Sweden
[b] Department of Chemistry and Biochemistry, University of California-Los Angeles, California 90095-1569, USA

ARTICLE INFO

Article history:
Received 19 December 2007
Received in revised form 14 March 2008
Accepted 17 March 2008
Available online 21 March 2008

Keywords:
Photosystem II
Oxygen evolving complex
S states
Split signals
EPR
Misses

ABSTRACT

EPR spectroscopy is very useful in studies of the oxygen evolving cycle in Photosystem II and EPR signals from the $CaMn_4$ cluster are known in all S states except S_4. Many signals are insufficiently understood and the S_0, S_1, and S_3 states have not yet been quantifiable through their EPR signals. Recently, split EPR signals, induced by illumination at liquid helium temperatures, have been reported in the S_0, S_1, and S_3 states. These split signals provide new spectral probes to the S state chemistry. We have studied the flash power dependence of the S state turnover in Photosystem II membranes by monitoring the split S_0, split S_1, split S_3 and S_2 state multiline EPR signals. We demonstrate that quantification of the S_1, S_3 and S_0 states, using the split EPR signals, is indeed possible in samples with mixed S state composition. The amplitudes of all three split EPR signals are linearly correlated to the concentration of the respective S state. We also show that the $S_1 \rightarrow S_2$ transition proceeds without misses following a saturating flash at 1 °C, whilst substantial misses occur in the $S_2 \rightarrow S_3$ transition following the second flash.

1. Introduction

Photosystem II (PSII) is a multisubunit protein complex which catalyses the light-driven oxidation of water into molecular oxygen and the reduction of plastoquinone in the thylakoid membrane of higher plants, green algae, and cyanobacteria [1–3]. A core part in this large enzyme is the OEC, which consists of a $CaMn_4$ cluster and a nearby redox-active tyrosine residue, Y_Z [4–9].

During the oxidation of two molecules of water to oxygen and protons, the OEC cycles through five intermediate redox states, collectively called S states, labelled S_0–S_4 [7–10]. The S_0 state is the most reduced state while the S_1, S_2 and S_3 states represent sequentially higher oxidation states. S_1 is the dominant state in a dark adapted sample, while S_2 and S_3 are metastable states that decay back to S_1 state in a few minutes at room temperature [11,12]. S_4 is a transient state involved in the formation and release of O_2 during $S_3 \rightarrow [S_4] \rightarrow S_0$ transition [7–9,13,14]. Starting from the dark stable S_1 state, oxygen is thus released upon the application of three short light flashes and thereafter every four flashes. All S states, except the transient S_4 state, can be trapped by exposing PSII samples to different numbers of laser flashes followed by rapid freezing [12].

EPR spectroscopy provides a useful means to study the oxidation states of the OEC of PSII. At present, EPR signals from the OEC in all trappable S states have been detected (for a recent review see [15]). The S_0 and S_2 states are paramagnetic, and display EPR signals from the $CaMn_4$ cluster under conventional perpendicular mode recording conditions. The S_2 state gives rise to the S_2 multiline signal, centred around $g=2$ and a broad EPR signal at $g=4.1$ [16–19], whereas the S_0 state also displays a multiline signal in the presence of a few percent of methanol [20,21]. The S_1 state EPR signals ($g=4.8$, 12) have been detected by using parallel mode EPR spectroscopy [22–25] while the S_3 state shows both broad parallel mode EPR signals ($g=8$, 12) and a perpendicular mode EPR signal at $g=6.7$ [26,27].

In recent years, several metalloradical EPR signals (split signals) attributed to the magnetic interaction between the oxidised Y_Z (Y_Z^{ox}) and the $CaMn_4$ cluster in PSII have been described from each of the S_1, S_2, S_3 and S_0 states when samples are illuminated with visible and/or NIR light at liquid helium temperatures [27–39]. The split S_1 and split S_3 signals are asymmetric: the former is characterised by a low-field peak at $g=2.035$ and the latter has a double trough at the high-field side of $g=2$ together with a weak broad peak at the low-field side. The split S_0 and split S_2 signals are more symmetric, with a significant low-field peak and a high-field trough centred around the $g=2$ region.

Studies of PSII and the mechanism of oxygen evolution often requires the trapping of PSII in the required S state by the application of laser flash(es) and rapid freezing of the sample. As a result, the

Abbreviations: Car, carotenoid; Chl, chlorophyll; Chl_Z, secondary chlorophyll electron donor to $P680^+$; Cytb_{559}, cytochrome b_{559}; EPR, electron paramagnetic resonance; DMSO, dimethylsulfoxide; MES, 2-(*N*-morpholino) ethanesulfonic acid; NIR, near-infrared; OEC, oxygen evolving complex; P680, primary electron donor chlorophylls in PSII; PpBQ, phenyl-*p*-benzoquinone; PSII, Photosystem II; Q_A and Q_B, primary and secondary plastoquinone acceptors of Photosystem II; Y_D, tyrosine 161 of the PSII D2 polypeptide; Y_Z, tyrosine 161 of the PSII D1 polypeptide

* Corresponding author. Tel.: +46 18 471 6580; fax: +46 18 471 6844.
E-mail address: stenbjorn.styring@fotomol.uu.se (S. Styring).

0005-2728/$ – see front matter © 2008 Elsevier B.V. All rights reserved.
doi:10.1016/j.bbabio.2008.03.007

sample obtained often contains a mixture of PSII centres in different S states due to, for example, misses in the S state transitions. In particular, this is important when high concentration PSII samples are needed, such as in for example EPR and X-ray spectroscopy experiments. In this study, we have used split EPR signals from the S_1, S_3, and S_0 states as well as the S_2 state multiline signal to quantify the distribution of centres in each S state after the application of varying numbers of laser flashes. Our research opens a new window for studies of turnover reactions in the OEC using high resolution spectroscopy.

2. Materials and methods

2.1. Preparation of PSII membranes

PSII-enriched membrane fragments were prepared under dim green light from deveined spinach leaves according to Berthold et al. [40], with modifications as in Völker et al. [41]. The stock PSII membranes (at ca 6–8 mg Chl/ml) were suspended in a buffer with 25 mM MES-NaOH (pH 6.3), 400 mM sucrose, 5 mM $MgCl_2$, 10 mM NaCl and stored at −80 °C before use. Under saturating continuous illumination, the oxygen evolution rate was 400±20 μmol of O_2 (mg of Chl)$^{-1}$h^{-1} in the presence of 0.5 mM PpBQ. The Chl concentration was determined in 80% ice-cold acetone according to the method of Arnon [42].

2.2. Synchronisation of the OEC to the S_1 state

PSII membranes diluted to 1.9–2.0 mg Chl/ml were filled in calibrated EPR tubes and illuminated with room light at 20 °C for 5 min to fully oxidise Y_D [43]. They were then dark incubated for 15 min at room temperature. The PSII centres were then synchronised to the S_1 state by the application of a preflash procedure followed by dark adaptation for a further 18 min at room temperature in the absence of electron acceptor [12,21,43].

2.3. Flash-induced turnover of the individual S states

To study the flash power dependence of the individual S state transitions, the exogenous electron acceptor PpBQ was added in the pre-flashed samples to a final concentration of 0.5 mM (from a stock solution in DMSO; final DMSO 3% v/v). 30 s after the addition of PpBQ, the samples were transferred to an ethanol bath at 1±1 °C and allowed to equilibrate for 3 min. After the equilibration, the samples were immediately given one, two or three flash(es) from a Nd: YAG laser (532 nm, 5 Hz, 6 ns, Spectra Physics, Newport, USA) with varying output power. After the turnover flashes, the samples were frozen in an ethanol–dry ice bath at 200 K within 1–2 s and then immediately transferred to liquid nitrogen where the samples were kept until EPR measurements. When indicated, the maximal induction of the S_2 state by the single laser flash was verified by subsequent continuous, saturating illumination at 200 K [12].

2.4. EPR measurement and low temperature illumination protocol

EPR measurements were performed with a Bruker ELEXYS E500 spectrometer using a SuperX EPR049 microwave bridge and a Bruker SHQ4122 cavity. The system was fitted with a liquid helium cryostat and temperature controller (ITC 503) from Oxford Instruments Ltd. Spectrometer settings are given in the figure legends.

The split EPR signals were induced by illumination directly into the EPR cavity at 5 K. Illumination with visible light was provided by a 150 W projector lamp fitted with a neutral density filter (10% T, Schott NG9) according to Zhang and Styring [33]. The light was filtered through a 5 cm thick $CuSO_4$ solution and directed into the EPR cavity using a transparent light guide. The intensity measured at the position of the cavity window was 160 W/m^2. NIR illumination at 830 nm was performed with a continuous laser diode (LQC830-135E laser diode, Newport, USA), with a beam-spreader lens placed in front of the EPR cavity window. The NIR light intensity applied on the EPR cavity window was 280 W/m^2. The complete procedure describing the sequence of events from the synchronisation preflash protocol to turnover flash(es) and low temperature illuminations to quantify the different S states is shown in Scheme 1. All EPR signal intensities were determined from measurements of their spectral amplitudes at defined magnetic field positions as described in the text and figures. The amplitudes were thereafter corrected for variations in sample volume and/or chlorophyll concentration using the non-saturated EPR signal from Y_D^{ox} as described in [44]. We estimate the precision of our amplitude measurements to be ±3% of the signal size.

3. Results and discussion

3.1. Time and light dependence of different split EPR signals induction

The split S_1 and split S_0 EPR signals are induced by illumination with visible light at 5 K. This illumination also induces a narrow radical EPR signal from competing oxidation of Car or Chl via the Car–Chl$_Z$–Cytb_{559} pathway [33–35,37–39]. The time dependence of the induction of the split S_0 and split S_1 signals under our particular illumination conditions (see Materials and methods) are shown in Fig. 1A. Both signals were quickly induced and reached the maximum amplitude after 4 min illumination with visible light.

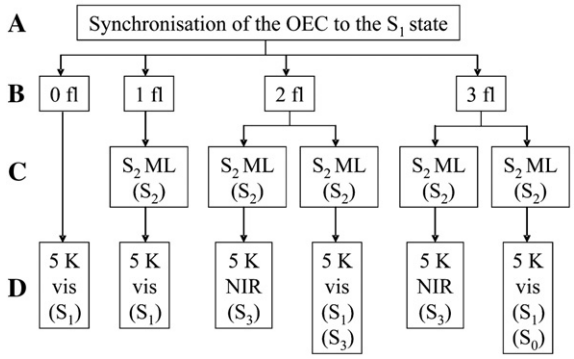

Scheme 1. Sequence of events leading to quantification of the S states. In parenthesis we show where a particular S state was quantified. A, Synchronisation of samples in the S_1 state was done according to [12,21,43]. B, Application of 0, 1, 2 or 3 turnover laser flash(es) in order to advance the samples to the S_1, S_2, S_3 or S_0 dominated state respectively. C, Measurements of the S_2 state multiline signal in order to quantify the S_2 state. D, Measurements of the split S_1 signal (after 0, 1, 2, or 3 turnover flash(es)), the split S_3 signal (after 2 turnover flashes) and the split S_0 signal (after 3 turnover flashes) in order to quantify the S_1, S_3, and S_0 states respectively. The signals were induced by visible light illumination at 5 K. In a parallel series of samples (after 2 and 3 turnover flashes) measurements of the split S_3 signal were performed in order to quantify the S_3 state. The signal was then induced by NIR illumination at 830 nm at 5 K.

The split S_3 signal can be induced with both visible and NIR light (Fig. 1B) [35]. With visible light, 60% of the maximum amplitude was formed after illumination for 4 min and the maximum was slowly reached after 60 min. The split S_3 signal was also induced at 5 K by light at 830 nm provided with a narrow band continuous laser diode and the maximum amplitude was reached after illumination for 60 min. When induced at this wavelength, the split S_3 signal is stable against fast decay [39] and is formed without interference from the Car–Chl$_Z$–Cytb_{559} pathway (which is not active at 830 nm). The maximum split S_3 signal obtained by illumination at 830 nm was ca 40% larger than the maximum signal obtained with visible light in an identical parallel sample (Fig. 1B, inset). There may be several reasons for this. Firstly, it reflects simultaneous formation and decay of the signal induced by visible light, whereas the signal induced by NIR light is stable in this time regime [39]. Secondly, it also reflects that the light at 830 nm penetrates deeper into the EPR sample than the visible light, which is efficiently absorbed by PSII centres in the outer layer of the EPR tube so that PSII centres in the middle are more difficult to excite [39]. It is also likely that the complex competing photochemistry from the Car–Chl$_Z$–Cytb_{559} pathway, which is only active in visible light, contributes.

The split EPR signals are induced in a light strength, wavelength [39] and temperature dependent manner. Except when the split S_3 signal is induced by NIR light, they also decay in the time scale of a few minutes at 5–10 K. Therefore, the balance between induction and decay governs the exact amplitude of the EPR signal (see above for the split S_3 signal). Therefore careful control of the exact details in the illumination protocol used to induce the respective split EPR signals is critical. In the experiments described here, we have chosen to illuminate the samples at 5 K during the entire EPR scan to minimise the importance of signal decay. Despite this, it is noteworthy that even using an optimal illumination protocol, it is possible that not all PSII centres in a particular S state are involved in the formation of the corresponding split EPR signal. Nevertheless, our careful control of the illumination conditions results in the same proportion of the respective split EPR signals being induced in response to the same induction conditions. The recorded EPR signal amplitudes can therefore be directly compared and used as

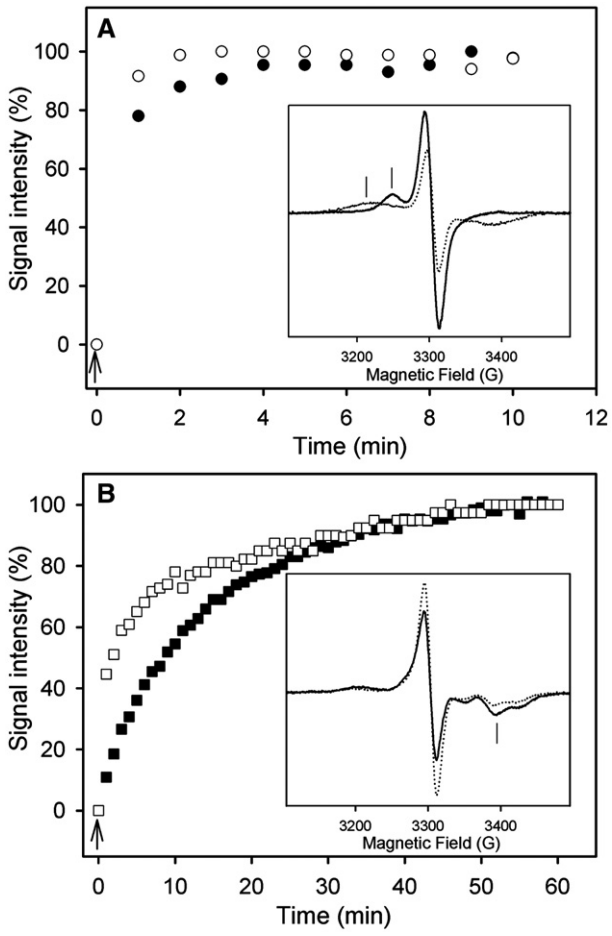

Fig. 1. Induction of the split EPR signals in different S states by illumination at 5 K. The EPR spectra shown are the light-minus-dark difference spectra between spectra recorded during illumination and spectra recorded before illumination. The induction kinetics was obtained by recording a new EPR spectrum every 60 s during the illumination and plotting the signal amplitude change against illumination time. (A) Induction of the split S_1 (○) and split S_0 (●) EPR signals with visible light, followed at 3250 G and 3220 G, respectively. The inset shows the split S_1 (solid line) and split S_0 signals (dotted line) induced by visible light illumination. (B) Induction of the split S_3 EPR signal by visible light (□) and NIR light at 830 nm (■) followed at 3393 G. The inset shows the split S_3 EPR signal induced by visible light illumination (dotted line) and NIR light at 830 nm (solid line) for 60 min. The bars in the inset spectra show the field positions used for data analysis. The arrows indicate the start of the illumination. The amplitudes plotted in A and B are normalised to the maximum signal (set to 100%) obtained in the respective experiments. EPR conditions: microwave power, 25 mW; microwave frequency, 9.27 GHz; modulation amplitude, 10 G; temperature, 5 K.

quantification tools for the particular S state. In our studies presented here we make use of this and in all experiments we apply either 4 min continuous illumination with visible light (for the split S_1, split S_3 and split S_0 signals) or 9 min illumination at 830 nm (for the split S_3 signal).

3.2. Concentration dependence of the split S_1 EPR signal amplitude

Fig. 2 shows the split S_1 EPR signals (Fig. 2A) induced by visible light illumination for 4 min at 5 K and the S_2 multiline EPR signals (Fig. 2B) recorded in samples given a single laser flash at different flash powers at 1±1 °C. In the dark (unflashed) sample, all PSII centres are in the S_1 state through the use of a preflash procedure that is considered to synchronise the absolute majority of the centres to the S_1 state [12,21,43]. This was verified in a sample which was studied after the preflash procedure without the application of turnover flashes. In this sample, the illumination at 5 K resulted in a large split S_1 signal while we could not observe any trace of the split S_0 signal. The sample was also completely devoid of the S_2 multiline signal (Fig. 2B, spectrum a). Thus the maximal split S_1 signal intensity (measured at 3250 G, Fig. 2A, spectrum a) represents 100% of the PSII centres. When one laser flash was applied, the induced split S_1 signal intensity decreased, whereas the S_2 state multiline signal intensity increased (Fig. 2B). The more intense the applied laser flash, the less intense the split S_1 signal became, and the more S_2 state multiline signal was observed. This reflects the advancement of the PSII centres in the S_1 state to the S_2 state.

When laser flashes at intermediate power were provided, this resulted in samples where both EPR signals could be observed as expected (Fig. 2A, spectra b, c and Fig. 2B spectra b, c), indicating incomplete turnover due to the non-saturating laser flash. When the laser flash was given at maximum output power (840 mJ), this resulted in the formation of the maximum S_2 multiline signal (Fig. 2B, spectrum d). Interestingly, the split S_1 signal was not detectable in the same sample, suggesting complete turnover of S_1 to S_2 by the single flash (Fig. 2A, spectrum d). We estimate the detection limit to be <5% of the maximum signal. To make this assignment clearer we have drawn a baseline in Fig. 2A. It can be seen that the prominent peak from the split S_1 signal (at 3250 G, Fig. 2A, spectrum a) is absent in spectrum d. Instead the spectrum contains a very small undulating signal. The identity of this signal is not known and attempts to further characterise this signal are in progress. It is clear that the application of the low power laser flash does not allow full turnover, which can by contrast be achieved at the highest flash power we have at our disposal.

The complete turnover in the $S_1 \rightarrow S_2$ transition obtained with maximal laser power under our experimental conditions could also be verified by measurement of the induction of the S_2 state by continuous illumination at 200 K. The S_2 state multiline signal has been widely studied and it is well established that its amplitude can be used for the quantification of S_2 state centres [12,17]. In such studies, a large S_2 multiline signal is observed after the application of one saturating laser flash, bringing most (or all, see below) S_1 centres to the S_2 state. Any centres remaining in the S_1 state after the flash can then be brought to the S_2 state by an additional illumination at 200 K. The combined S_2 multiline signal is then considered to represent 100% of the PSII centres [12,45]. When the laser flash is provided at 20–25 °C, the subsequent illumination at 200 K normally results in an increase of 10±5% in the amplitude of the S_2 multiline signals [12,21,45–47], indicating a substantial fraction of misses.

We performed this experiment on our synchronised PSII samples. Interestingly, the amplitude of the S_2 multiline induced by the single laser flash provided at 1±1 °C with maximal flash power (840 mJ) (Fig. 2B, spectrum d) did not increase after additional illumination at 200 K (Fig. 2B, spectrum e). This is a strong indication that no PSII centres remained in the S_1 state after the powerful laser flash. In this case it should also be mentioned that no $g=4.1$ signal from the S_2 state was induced either by our flash protocol or by the subsequent illumination at 200 K (supplementary Figure A).

Thus, we arrive at the same conclusion that there are no misses in the $S_1 \rightarrow S_2$ transition at 1±1 °C both from the measurement of the S_2 multiline signal formed and the disappearance of the split S_1 signal. Consequently, the S_2 multiline signal intensity induced by a single saturating flash at 1±1 °C represents 100% of the PSII centres being in the S_2 state, and all other S_2 multiline signal amplitudes are scaled to this value.

We also attempted to use the amplitude of the split S_1 signal as a new probe of the concentration of the S_1 state. Fig. 2C shows the flash power dependence of the formation of the S_2 state (as measured by the S_2 multiline signal) and the disappearance of the S_1 state (as measured by the split S_1 signal). The maximum intensity of the split S_1 signal induced in the synchronised, unflashed sample and the S_2 multiline EPR signal in the one-flash sample correspond to 100% of the PSII centres being in the S_1 state and the S_2 state respectively. Therefore, the signal intensities in samples containing a mixture of S_1 and S_2 state centres could be used to calculate the proportion of the S_1 and S_2 states.

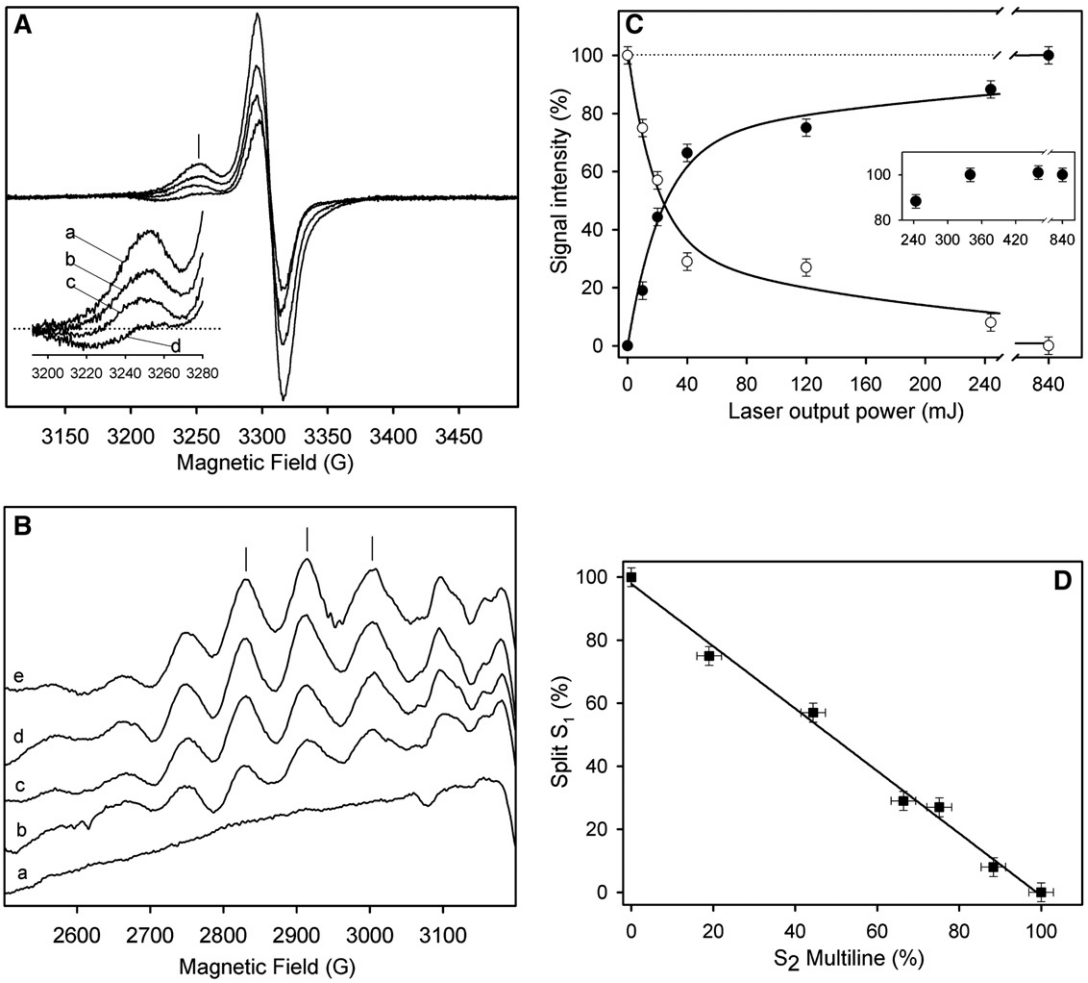

Fig. 2. Efficiency of the $S_1 \rightarrow S_2$ transition at 1 ± 1 °C in samples provided with one flash with different laser power. (A) Split S_1 EPR signal induced by visible light illumination for 4 min at 5 K in samples given one laser flash at output powers of 0 mJ = dark (a), 20 mJ (b), 120 mJ (c), and 840 mJ (d). The spectra are light-minus-dark difference spectra. EPR conditions: microwave power, 25 mW; microwave frequency, 9.27 GHz; modulation amplitude, 10 G; temperature, 5 K. (B) S_2 multiline EPR signals (only the low-field part of the EPR spectra is shown) from samples exposed to one laser flash at output powers of 0 mJ = dark (a), 20 mJ (b), 120 mJ (c), and 840 mJ (d). Spectrum e was obtained by continuous illumination of sample d at 200 K for 5 min. EPR conditions: microwave power, 10 mW; microwave frequency, 9.27 GHz; modulation amplitude, 20 G; temperature, 10 K. Peaks used to estimate the amplitude of the EPR signals are indicated by the bars. (C) Normalised amplitudes showing the laser flash power dependence of the signal intensities of the split S_1 (○) and S_2 multiline EPR signals (●). The split S_1 signal in the dark (0 mJ, Fig. 2A, a) and the maximally obtained S_2 multiline signal (840 mJ, Fig. 2B, d) are set to 100%, respectively (dotted line). The inset shows the amplitudes of S_2 multiline signal induced at output powers between 240 mJ and 840 mJ. (D) Correlation of the split S_1 signal induced by 5 K illumination and S_2 multiline signal after the application of one flash at different laser power at 1 ± 1 °C.

The validity of this approach was verified by the inverse linear correlation between the intensities of the split S_1 and S_2 multiline EPR signals measured in the same sample (Fig. 2D). This is a useful result and indicates that both EPR signals can be used to determine the fraction of PSII present in the respective S state. This was known before in the case of the S_2 multiline signal but has so far not been demonstrated for the split S_1 EPR signal.

In summary, the S_1 split signal could be used as a probe for S_1 state centres in samples containing a mixture of S_1 and S_2 state centres. It was also found that the application of one saturating flash to an S_1 synchronised sample at 1 ± 1 °C gave 100% induction of S_2 centres. This is an important result, indicating that the $S_1 \rightarrow S_2$ transition does not involve any kind of misses or back reactions under these conditions. To the best of our knowledge, this is the first clear example of an S state transition occurring without misses.

3.3. Concentration dependence of the split S_3 EPR signal amplitude

The application of two laser flashes at 1 ± 1 °C resulted in the appearance of both the S_2 and S_3 states (Fig. 3). The S_2 state was probed by the S_2 multiline signal (see above) while the remaining centres in the S_1 and S_3 states were probed by their respective split signals. The split EPR signals were induced by visible light illumination for 4 min in the two-flash samples and the observed split EPR signals reflect a mixture of PSII centres in the S_1 and S_3 states (Fig. 3A). Increasing the power of the flash, the sample successively became dominated by the S_3 state, though with some PSII centres always remaining in the S_1 and/or S_2 states. In these spectra, the high-field trough (3393 G) is free from split S_1 and was used to analyse the S_3 state.

The analysis of the split S_1 signal was complicated, since the split S_3 signal gives rise to a low-field peak centred at 3205 G which partly overlaps with the split S_1 peak as seen in the split S_3 signal obtained by NIR illumination at 830 nm (Fig. 3A, spectrum e). Since the S_1 split signal is not induced by NIR illumination at 5 K (not shown), the split S_3 signal induced in this manner can be regarded as a "clean" split S_3 signal. Therefore, the analysis of the split S_1 signal in mixed EPR spectra can be achieved by subtraction of a weighted fraction of the NIR-induced split S_3 signal. The high-field side of the split S_3 signal in the mixed spectra, which does not overlap with any part of the split S_1 signal, is used as a scaling reference.

In samples exposed to laser flashes at lower power (e. g. 20 mJ, Fig. 3A, spectrum b), the sample contained a considerable fraction of

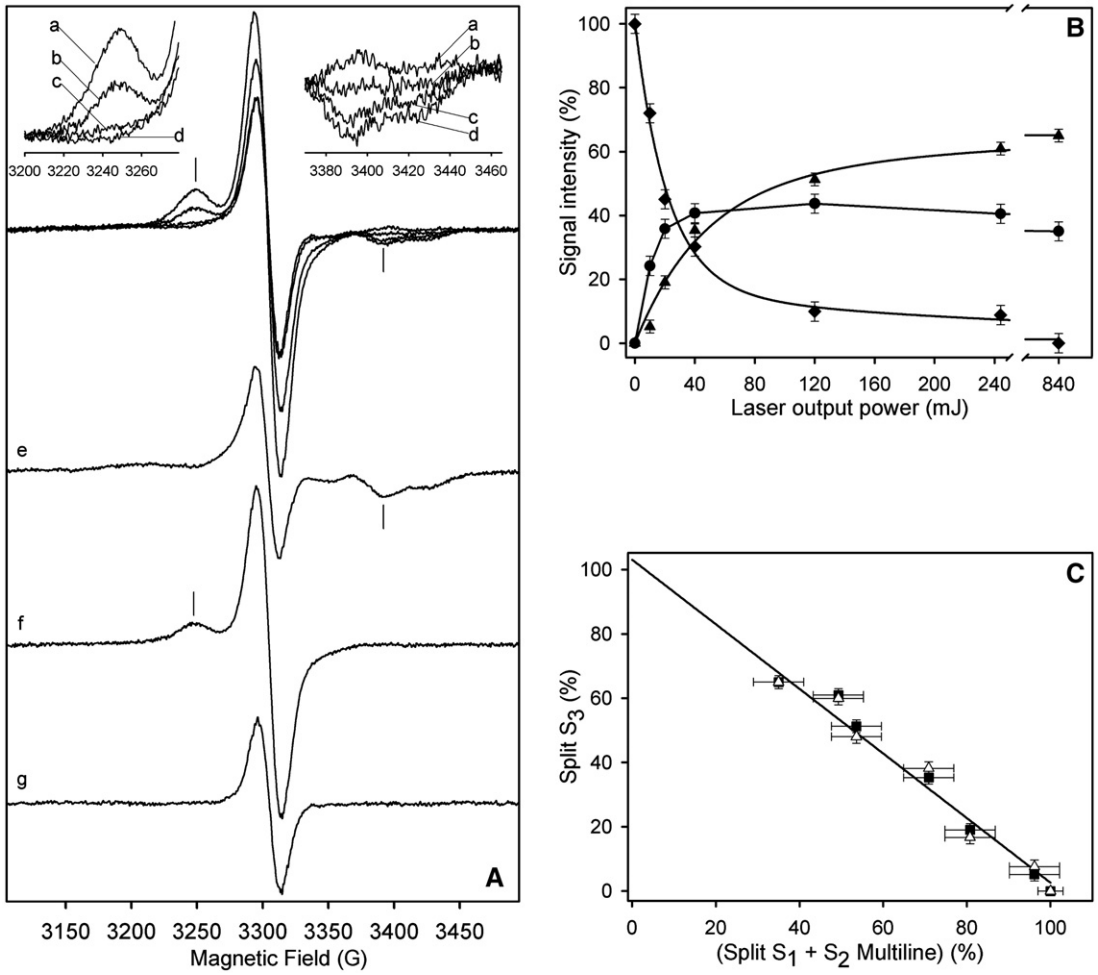

Fig. 3. Efficiency of the formation of the S_3 state at 1 ± 1 °C with two flashes at different laser power. (A) Split EPR signals induced by illumination at 5 K of samples given two laser flashes at output powers of 0 mJ = dark (a), 20 mJ (b), 120 mJ (c), and 840 mJ (d, e). The spectra are light-minus-dark difference spectra. Spectra a–d were induced by illumination for 4 min with visible light while spectrum e shows the split S_3 EPR signal induced by continuous laser light at 830 nm for 9 min. Spectra f and g were obtained by subtraction of a weighted fraction of the "clean" split S_3 signal (spectrum e) from spectra b and d respectively, based on the size of the high-field troughs. The bars indicate the peak (3250 G) and trough (3393 G) used to estimate the amplitude of the split EPR signals. EPR conditions were as in Fig. 2A. (B) Normalised amplitudes showing the laser flash power dependence of the relative signal intensities of the split S_1 (◆), the S_2 multiline (●) (spectra not shown) and the split S_3 (▲) EPR signals. The amplitudes of the split S_1 signal in the dark sample and the S_2 multiline after one saturating flash at 1 ± 1 °C represent 100% of PSII. The amplitude of the split S_3 signal in the sample given two saturating flashes (840 mJ) represents 65% of PSII (see the text for discussion). (C) Correlation of the relative percentage of PSII in the S_3 state determined from the split S_3 signal and the summed fraction of PSII in the S_1 and S_2 states determined from the split S_1 and S_2 multiline signals in samples given two flashes at different power at 1 ± 1 °C. The correlation is shown for the split S_3 signal induced by visible light illumination for 4 min (■) or by NIR light illumination for 9 min at 830 nm (△).

the S_1 state as judged by the observation of the split S_1 signal in the deconvoluted spectrum (Fig. 3A, spectrum f). This allows quantification of the S_1 state by comparison to the split S_1 signal in the zero-flash sample, which represented 100% of PSII (see above).

After two flashes at maximum output power (840 mJ), the resulting EPR spectrum after subtraction of the split S_3 signal is shown in Fig. 3A, spectrum g. There is no observable split S_1 signal in this spectrum. Thus, only the S_2 and S_3 states are present after the two flashes at maximum flash power. This is in agreement with the conclusion above that the $S_1 \rightarrow S_2$ turnover is complete upon the application of a laser flash at full power at 1 ± 1 °C. The PSII centres in the S_2 state can be quantified with the S_2 multiline signal (see above) while the remaining PSII centres give rise to the split S_3 signal. After two flashes at maximum output power, the analysis of the S_2 multiline signal revealed that 35% of the PSII centres were in the S_2 state (not shown). Consequently, the recorded split S_3 signal (Fig. 3A, spectrum d) represents 65% of the PSII centres. Using this value, the relative fraction of PSII centres in the S_3 state was calculated from the intensity of the split S_3 signal in all mixed samples.

Based on this information, the fractions of the S_1, S_2 and S_3 states could be quantified in the samples obtained after exposure to the non-saturating laser flashes (Fig. 3B). With increasing laser flash power, the S_3 state (as measured by the split S_3 signal) involves an increasing fraction of PSII centres while the fraction of S_1 centres (as measured by the split S_1 signal) decreased, completely vanishing at the maximum flash power. However, the observation that a substantial fraction of the S_2 state (as measured by the S_2 multiline signal) is present even after two flashes at the highest power indicates that a substantial miss occurs in the second flash. This is an important observation and indicates a very S state dependent miss pattern at 1 ± 1 °C.

We also investigated whether the split S_3 signal can be used to determine the concentration of the S_3 state. This was done by plotting the fraction of PSII in the S_3 state against the summed fractions of PSII in the S_1 and S_2 states (data from Fig. 3B). The result is shown in Fig. 3C. The linear inverse correlation demonstrates that the amplitude of the split S_3 signal can be used as a spectroscopic probe to quantify the S_3 state.

The same holds for the "clean" split S_3 signal induced by NIR light at 830 nm (Fig. 3C). Thus, despite the fact that the maximal split S_3 signal obtained by NIR light was bigger than the signal obtained by visible light (Fig. 1B), both signals could be used to probe the fraction of the centres in the S_3 state. This also proves our concept that, provided that the illumination scheme is carefully controlled, the split signals are a useful probe to quantify the various S states.

3.4. Concentration dependence of the split S_0 EPR signal amplitude

Fig. 4 shows the laser flash power dependence of the S state dependent EPR signals in PSII samples given three flashes at 1 ± 1 °C. In samples exposed to three flashes, the S_0 state was reached, but some PSII centres still remained in the S_1, S_2 and S_3 states. The fraction in the S_2 state could be determined from the S_2 multiline signal as before. However, the EPR spectrum recorded after visible light illumination for 4 min at 5 K contained a mixture of the split S_0, split S_1 and split S_3 EPR signals (Fig. 4A, spectra a–d) [37–39].

Due to the simultaneous presence of all of these S states in the sample, the analysis is more complex than for one- or two-flash samples. To facilitate the analysis, the split S_3 signal was first quantified by selectively inducing it with illumination at 830 nm in a parallel series (three laser flashes at similar laser powers). The proportion of PSII in the S_3 state was then obtained by comparison of these spectra with the NIR-induced split S_3 signal from a sample exposed to two saturating flashes where 65% of PSII was in the S_3 state (Fig. 3A, spectrum e).

Using these quantifications for scaling, the contribution of the split S_3 signal could then be removed from to the visible light induced mixed split signal spectra (Fig. 4A) by weighted subtraction of the "pure" visible light induced split S_3 signal (Fig. 3A, spectrum d). The resulting EPR spectra, while still mixed, contain only contributions from the split S_0 and/or the split S_1 EPR signals. Examples of these spectra are shown in Fig. 4A (f, g). Note that the extracted spectrum from the sample provided with three saturating flashes (laser power at 840 mJ) did not contain any contribution from the S_1 state (Fig. 4A spectrum f) again consistent with the result that one saturating flash results in complete $S_1 \rightarrow S_2$ turnover. Hence, this spectrum represents the "pure" split S_0 signal induced from the PSII centres that reached the S_0 state with three saturating flashes.

The results in this experiment show that the S state composition in a sample exposed to three saturating flashes is 21% in the S_2 state and 24% in the S_3 state as determined from the S_2 state multiline (not shown) and split S_3 signals, respectively. Thus, the maximal split S_0 EPR signal (Fig. 4A, spectrum f) represented 55% of PSII. This type of

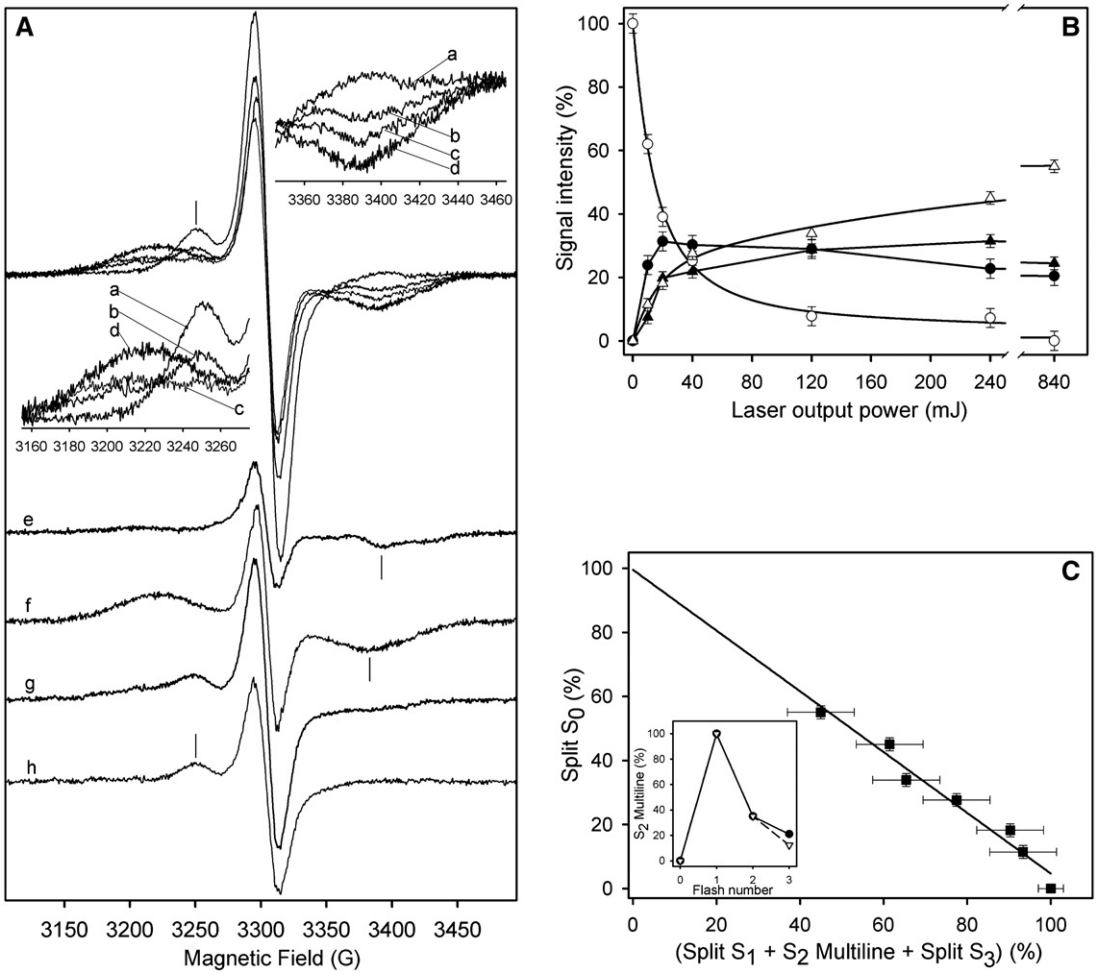

Fig. 4. Efficiency of the formation of the S_0 state at 1 ± 1 °C with three flashes at different laser power. (A) Split EPR signals induced by illumination at 5 K in samples given three flashes at output powers of 0 mJ = dark (a), 20 mJ (b),120 mJ (c), and 840 mJ (d), (e). The spectra are light-minus-dark difference spectra. Spectra a–d were induced by illumination with visible light for 4 min while spectrum e is the split S_3 signal induced by NIR light for 9 min at 830 nm. Spectra f and g are the spectra obtained by subtracting a weighted fraction of the split S_3 signal from spectra d and b respectively. Therefore, spectrum f shows the "pure" split S_0 signal after three flashes at high laser power (840 mJ) while spectrum g contains a mixture of the split S_0 and split S_1 signals due to the low laser power applied (20 mJ). Spectrum h is obtained by subtracting the weighted split S_0 signal (from spectrum f) from spectrum g with the high-field trough as reference. The bars indicate the peaks (split S_1, 3250 G) and troughs (split S_3, 3393 G; split S_0, 3382 G) used to estimate the amplitude of the different split EPR signals. EPR conditions were as in Fig. 2A. (B) Normalised amplitudes showing the laser flash power dependence of the relative signal intensities of the split S_1 (○), S_2 multiline (●) (spectra not shown), split S_3 (▲) and split S_0 (△) signals. The amplitude of the split S_1 signal in the dark sample and the S_2 multiline after one saturating flash at 1 ± 1 °C are set to represent 100% of PSII. The amplitudes of the split S_3 signal in a sample given two saturating flashes (840 mJ) and the split S_0 signal in a sample given three saturating flashes (840 mJ) represent 65% and 55% of the PS II centres respectively (see text for explanation). (C) Correlation of the relative percentage of PSII in the S_0 state determined from the split S_0 signal amplitude and the combined fractions of PSII in the S_2, S_1 and S_3 states determined from respectively the S_2 multiline, split S_1 and the split S_3 signals recorded in samples exposed to three flashes with different laser powers. The inset shows the flash-dependent oscillation pattern of the S_2 multiline EPR signal (●) and fit (▽), assuming the same miss parameter (35%) on the $S_2 \rightarrow S_3$ transition both in the 2nd and 3rd flash. The flashes were given at 5 Hz (840 mJ, 532 nm) and 1 ± 1 °C.

correlation between the size of the split S_0 signal (or any other EPR signal from the S_0 state) and the fraction of PSII centres in the S_0 state in a mixed S state sample has not been attempted before.

We therefore tested if we could use the split S_0 signal to determine the fraction of S_0 in samples where this varied due to the use of varying laser power. As above, subtraction of the contribution from the split S_3 signal results in EPR spectra that contain a mixture of the split S_1 and split S_0 signals. Since the high-field trough (3382 G) in these spectra is free from contributions from the split S_1 signal (c.f. Fig. 2A), this was used to analyze the S_0 state. Using the maximal pure split S_0 signal as a scaling reference (corresponding to 55% of PSII, see above), the contribution from the split S_0 signal was removed by weighted subtraction. This resulted in spectra with a "clean" split S_1 signal (Fig. 3A, h), which in turn allowed determination of the S_1 state by comparison with the split S_1 signal in the unflashed sample (representing 100% of PSII).

Fig. 4B shows the quantitative analysis of the S state composition in samples exposed to three laser flashes at varying power using EPR spectra similar to those in Fig. 4A and EPR spectra of the S_2 multiline signal (not shown). It is seen that, with the laser flash power increasing, the S_0 state became dominating in the PSII sample. Only at very high flash power did the laser light not seem to be the limiting factor.

The data in Fig. 4B were used to investigate whether the size of the split S_0 signal could also be used to quantify the S_0 state. The plot clearly shows that the fraction of centres in the S_0 state, determined from the normalised amplitude of the split S_0 signal, is linearly and inversely correlated to the combined fraction of PSII centres present in the S_1, S_2 and S_3 states (Fig. 4C). Thus, it is possible to use the relative amplitude of the split S_0 signal for quantitative analysis of the fraction of PSII present in the S_0 state.

It is most difficult to determine the distribution of the different S states in the three-flash samples since they contain PSII centres in the S_2, S_3, and S_0 states and, potentially, in the S_1 state. The reasons for this mixed distribution are the misses which occur on the $S_2 \rightarrow S_3$ and $S_3 \rightarrow S_0$ transitions while there is no miss in the $S_1 \rightarrow S_2$ transition. The inset in Fig. 4C shows the oscillation pattern of the S_2 multiline EPR signal in the PSII samples after 0, 1, 2 and 3 saturating laser flashes given at 5 Hz frequency and 1±1 °C. We observed that 35% and 21% of the S_2 multiline signal remained after the second and third flash respectively (Figs. 3B, 4B and inset in Fig. 4C). As discussed above this indicates that a significant miss (35%) occurs on the $S_2 \rightarrow S_3$ transition. Our fitting using the same miss parameter (35%) for both the second and the third flash indicates that a lower fraction (12%) of the PSII centres should have remained in the S_2 state after the third flash as compared to the measured fraction (21%). Seemingly, the third flash does not turn these PSII centres remaining in the S_2 state over with the same efficiency. At first glance this suggests that a fraction of the PSII centers is stuck in the S_2 state as was observed before [48,49]. However, an alternative explanation, which we prefer, reflects limitations in the electron transfer on the acceptor side of PSII due to the low temperature (1± 1 °C) in the experiment. If this is the case, the flash advancement on the second and third flash (and thereafter) would occur with higher efficiency at lower flash frequencies. Experiments to test this hypothesis are in progress.

4. Conclusions

In this study, we have attempted to quantify the PSII centres in all S states through the use of the recently discovered split EPR signals from the S_0, S_1 and S_3 states, induced by illumination at 5 K, and the well-studied S_2 state multiline signal. This is an improvement compared to earlier EPR studies and many X-ray studies where only the S_2 state could be followed using the S_2 state multiline signal [47–50]. The results demonstrate that these split EPR signals provide a novel probe to study the S state transitions individually that is more direct than the commonly used analysis of flash-dependent oxygen yield measurements.

At present, there are no other direct methods available for the study of distribution of the S states using the same experimental technique. Therefore, investigations of the S state cycle using these EPR spectroscopy probes provide a new opportunity to study the individual S-transitions and S-cycle efficiency. In addition, by varying other parameters such as temperature and pH, it will be possible to follow how the particular S-state transition and back reactions are affected. In this way, new information on the kinetics and thermodynamics of the PSII water-oxidizing mechanism could be gained. We are presently conducting a study on the temperature dependence of the misses in the different S state transitions. This has been triggered by the interesting observation that the $S_1 \rightarrow S_2$ transition proceeds without any misses at 1±1 °C.

Acknowledgements

The financial support from the Swedish Research Council, the Swedish Energy Agency, the Knut and Alice Wallenberg Foundation and the European Community Sixth Framework Programme, Marie Curie Incoming International Fellowship (514817 to FMH) is gratefully acknowledged. Drs Ji-Hu Su (Mü lheim an der Ruhr, Germany) and Yashar Feyziyev (Baku, Azerbaijian) are gratefully acknowledged for helpful discussions.

Appendix A. Supplementary data

Supplementary data associated with this article can be found, in the online version, at doi:10.1016/j.bbabio.2008.03.007.

References

[1] J. Barber, Photosystem II: the engine of life, Q. Rev. Biophys. 36 (2003) 71–89.
[2] N. Nelson, C.F. Yocum, Structure and function of photosystems I and II, Annu. Rev. Plant Biol. 57 (2006) 521–565.
[3] T. Wydrzynski, K. Satoh (Eds.), Photosystem II: The Light Driven Water: Plastoquinone Oxidoreductase, Springer, The Netherlands, 2005.
[4] N. Kamiya, J.R. Shen, Crystal structure of oxygen evolving photosystem II from *Thermosynechococcus vulcanus* at 3.7 Å resolution, Proc. Natl. Acad. Sci. U. S. A. 100 (2003) 98–103.
[5] K.N. Ferreira, T.M. Iverson, K. Maghlaoui, J. Barber, S. Iwata, Architecture of the photosynthetic oxygen evolving center, Science 303 (2004) 1831–1838.
[6] B. Loll, J. Kern, W. Saenger, A. Zouni, J. Biesiadka, Towards complete cofactor arrangement in the 3.0 Å resolution structure of photosystem II, Nature 438 (2005) 1040–1044.
[7] G. Renger, Photosynthetic water oxidation to molecular oxygen: apparatus and mechanism, Biochim. Biophys. Acta 1503 (2001) 210–228.
[8] C. Goussias, A. Boussac, A.W. Rutherford, Photosystem II and photosynthetic oxidation of water: an overview, Philos. Trans. R. Soc. Lond., B 357 (2002) 1369–1381.
[9] J.P. McEvoy, G.W. Brudvig, Water-splitting chemistry of photosystem II, Chem. Rev. 106 (2006) 4455–4483.
[10] B. Kok, B. Forbush, M. McGloin, Cooperation of charges in photosynthetic O_2 evolution — I. A linear four-step mechanism, Photochem. Photobiol. 11 (1970) 457–475.
[11] B. Forbush, B. Kok, M.P. McGloin, Cooperation of charges in photosynthetic O_2 evolution — II. Damping of flash yield oscillation, deactivation, Photochem. Photobiol. 14 (1971) 307–321.
[12] S. Styring, A.W. Rutherford, Deactivation kinetics and temperature dependence of the S-states transition in the oxygen-evolving system of photosystem II measured by EPR spectroscopy, Biochim. Biophys. Acta 933 (1988) 378–387.
[13] J. Clausen, W. Junge, Detection of an intermediate of photosynthetic water oxidation, Nature 430 (2004) 480–483.
[14] M. Haumann, P. Liebisch, C. Muller, M. Barra, M. Grabolle, H. Dau, Photosynthetic O_2 formation tracked by time resolved X-ray experiments, Science 310 (2005) 1019–1021.
[15] A. Haddy, EPR spectroscopy of the manganese cluster of photosystem II, Photosynth. Res. 92 (2007) 357–368.
[16] G.C. Dismukes, Y. Siderer, Intermediates of a polynuclear manganese center involved in photosynthetic oxidation of water, Proc. Natl. Acad. Sci. U. S. A. 78 (1981) 274–278.
[17] G.W. Brudvig, J.L. Casey, K. Sauer, The effect of temperature on the formation and decay of the multiline EPR signal species associated with photosynthetic oxygen evolution, Biochim. Biophys. Acta 723 (1983) 366–371.
[18] J.L. Casey, K. Sauer, EPR detection of a cryogenically photogenerated intermerdiate in photosynthetic oxygen evolution, Biochim. Biophys. Acta 767 (1984) 21–28.
[19] J.L. Zimmermann, A.W. Rutherford, EPR studies of the oxygen-evolving enzyme of photosystem II, Biochim. Biophys. Acta 767 (1984) 160–167.
[20] J. Messinger, J.H.A. Nugent, M.C.W. Evans, Detection of an EPR multiline signal for the S_0* state in photosystem II, Biochemistry 36 (1997) 11055–11060.

[21] K.A. Åhrling, S. Peterson, S. Styring, An oscillating manganese electron paramagnetic resonance signal from the S_0 state of the oxygen evolving complex in photosystem II, Biochemistry 36 (1997) 13148–13152.
[22] S.L. Dexheimer, M. P Klein, Detection of a paramagnetic intermediate in the S_1 state of the photosynthetic oxygen evolving complex, J. Am. Chem. Soc. 114 (1992) 2821–2826.
[23] T. Yamauchi, H. Mino, T. Matsukawa, A. Kawamori, T.A. Ono, Parallel polarization electron paramagnetic resonance studies of the S_1-state manganese cluster in the photosynthetic oxygen evolving system, Biochemistry 36 (1997) 7520–7526.
[24] K.A. Campbell, W. Gregor, D.P. Pham, J.M. Peloquin, R.J. Debus, R.D. Britt, The 23 and 17 kDa extrinsic proteins of photosystem II modulate the magnetic properties of the S_1-state manganese cluster, Biochemistry 37 (1998) 5039–5045.
[25] K.A. Campbell, J.M. Peloquin, D.P. Pham, R.J. Debus, R.D. Britt, Parallel polarization EPR detection of an S_1-state "multiline" EPR signal in photosystem II particles from *Synechocystis* sp.PCC 6803, J. Am. Chem. Soc. 120 (1998) 447–448.
[26] T. Matsukawa, H. Mino, D. Yoneda, A. Kawamori, Dual-mode EPR study of new signals from the S_3-state of oxygen-evolving complex in photosystem II, Biochemistry 38 (1999) 4072–4077.
[27] N. Ioannidis, V. Petrouleas, Electron paramagnetic resonance signals from the S_3 state of the oxygen-evolving complex. A broadened radical signal induced by low-temperature near infrared light illumination, Biochemistry 39 (2000) 5246–5254.
[28] J.H.A. Nugent, S. Turconi, M.C.W. Evans, EPR investigation of water oxidizing photosystem II: detection of new EPR signals at cryogenic temperatures, Biochemistry 36 (1997) 7086–7096.
[29] N. Ioannidis, V. Petrouleas, Decay products of the S_3 state of the oxygen-evolving complex of Photosystem II at cryogenic temperatures. Pathways to the formation of the S = 7/2 S_2 state configuration, Biochemistry 41 (2002) 9580–9588.
[30] N. Ioannidis, J.H.A. Nugent, V Petrouleas, Intermediates of the S_3 state of the oxygen-evolving complex of photosystem II, Biochemistry 41 (2002) 9589–9600.
[31] J.H.A. Nugent, I.P. Muhiuddin, M.C.W. Evans, Electron transfer from the water oxidizing complex at cryogenic temperatures: The S_1 to S_2 step, Biochemistry 41 (2002) 4117–4126.
[32] D. Koulougliotis, J.R. Shen, N. Ioannidis, V. Petrouleas, Near-IR irradiation of the S_2 state of the water oxidizing complex of photosystem II at liquid helium temperatures produces the metalloradical intermediate attributed to $S_1Y_Z^{\cdot}$, Biochemistry 42 (2003) 3045–3053.
[33] C. Zhang, S. Styring, Formation of split electron paramagnetic resonance signals in photosystem II suggests that tyrosine Z can be photooxidized at 5 K in the S_0 and S_1 states of the oxygen-evolving complex, Biochemistry 42 (2003) 8066–8076.
[34] C. Zhang, A. Boussac, A.W. Rutherford, Low temperature electron transfer in photosystem II: a tyrosyl radical and semiquinone charge pair, Biochemistry 43 (2004) 13787–13795.
[35] D. Koulougliotis, C. Teutloff, Y. Sanakis, W. Lubitz, V. Petrouleas, $S_1Y_Z^{\cdot}$ metalloradical intermediate in photosystem II: an X- and W-band EPR study, Phys. Chem. Chem. Phys. 6 (2004) 4859–4863.
[36] N. Ioannidis, G. Zahariou, V. Petrouleas, Trapping of the S_2 to S_3 state intermediate of the oxygen-evolving complex of photosystem II, Biochemistry 45 (2006) 6252–6259.
[37] J.-H. Su, K.G.V. Havelius, F. Mamedov, F.M. Ho, S. Styring, Split EPR signals from photosystem II are modified by methanol, reflecting S state-dependent binding and alterations in the magnetic coupling in the $CaMn_4$ cluster, Biochemistry 45 (2006) 7617–7627.
[38] K.G.V. Havelius, J.-H. Su, Y. Feyziyev, F. Mamedov, S. Styring, Spectral resolution of the split EPR signals induced by illumination at 5 K from the S_1-, S_3- and S_0-states in photosystem II, Biochemistry 45 (2006) 9279–9290.
[39] J.-H. Su, K.G.V. Havelius, F.M. Ho, G. Han, F. Mamedov, S. Styring, Formation spectra of the EPR split signals from the S_0, S_1, and S_3 states in photosystem II induced by monochromatic light at 5 K, Biochemistry 46 (2007) 10703–10712.
[40] D.A. Berthold, G. T Babcock, C.F. Yocum, A highly resolved, oxygen-evolving photosystem II preparation from spinach thylakoid membranes, FEBS Lett. 134 (1981) 231–234.
[41] M. Völker, T. Ono, Y. Inoue, G. Renger, Effect of trypsin on PS-II particles. Correlation between Hill-activity, Mn abundance and peptide pattern, Biochim. Biophys. Acta 806 (1985) 25–34.
[42] D.I. Arnon, Copper enzymes in isolated chloroplasts. Polyphenoloxidase in *Beta vulgaris*, Plant Physiol. 24 (1949) 1–15.
[43] S. Styring, A.W. Rutherford, In the oxygen-evolving complex of photosystem II the S_0 state is oxidized to the S_1 state by D^+ (Signal II $_{slow}$), Biochemistry 26 (1987) 2401–2405.
[44] Bernát, Morvaridi, Y. Feyziyev, S. Styring, pH dependence of the four individual transitions in the catalytic S-cycle during photosynthetic oxygen evolution, Biochemistry 41 (2002) 5830–5843.
[45] S.F. Morvaridi, Y. Feyziyev, S. Styring, Effect of temperature on the miss-factor in the S-cycle determined by EPR, in: A. van der Est, D. Bruce (Eds.), Photosynthesis: Aspects to Global Perspectives, Alliance Communications Group, Lawrence, KS, 2005, pp. 359–360.
[46] F.M. Ho, S.F. Morvaridi, F. Mamedov, S. Styring, Enhancement of Y_D spin relaxation by the $CaMn_4$ cluster in photosystem II detected at room temperature: a new probe for the S-cycle, Biochim. Biophys. Acta 1767 (2007) 5–14.
[47] T.A. Roelofs, W. Liang, M.J. Latimer, R.M. Cinco, A. Rompel, J.C. Andrews, K. Sauer, V.K. Yachandra, M.P. Klein, Oxidation states of the manganese cluster during the flash-induced S-state cycle of the photosynthetic oxygen-evolving complex, Proc. Natl. Acad. Sci. U. S. A. 93 (1996) 3335–3340.
[48] J. Messinger, J.H. Robblee, U. Bergmann, C. Fernandez, P. Glatzel, H. Visser, R.M. Cinco, K.L. McFarlane, E. Bellacchio, S.A. Pizarro, S.P. Cramer, K. Sauer, M.P. Klein, V.K. Yachandra, Absence of Mn-centered oxidation in the $S_2 \rightarrow S_3$ transition: implications for the mechanism of photosynthetic water oxidation, J. Am. Chem. Soc. 123 (2001) 7804–7820.
[49] M. Haumann, C. Müller, P. Liebisch, L. Iuzzolino, J. Dittmer, M. Grabolle, T. Neisius, W. Meyer-Klaucke, H. Dau, Structural and oxidation state changes of the photosystem II manganese complex in four transitions of the water oxidation cycle ($S_0 \rightarrow S_1$, $S_1 \rightarrow S_2$, $S_2 \rightarrow S_3$, and $S_{3,4} \rightarrow S_0$) characterized by X-ray absorption spectroscopy at 20 K and room temperature, Biochemistry 44 (2005) 1894–1908.
[50] L. Iuzzolino, J. Dittmer, W. Dörner, W. Meyer-Klaucke, H. Dau, X-ray absorption spectroscopy on layered photosystem II membrane particles suggests manganese-centered oxidation of the oxygen-evolving complex for the S_0-S_1, S_1-S_2, and S_2-S_3 transitions of the water oxidation cycle, Biochemistry 37 (1998) 17112–17119.